BJES Basrah Journal for Engineering Sciences

Basrah Journal for Engineering Sciences, Vol. 23, No. 1, (2023), 81-89

Original Article

Journal homepage: www.bjes.edu.iq
ISSN (Online): 23118385, ISSN (Print): 18146120

OPEN ACCESS

Numerical Simulation of the Aerodynamic Characteristics of NACA0012 Airfoil Based on Operational Parameters

Ayat A. Mula [1, *], Mohammed A. Abdulwahid [2]

[1, 2] *Department of Thermal Mechanical Technical Engineering, Southern Technical University, Basrah, Iraq*
E-mail addresses: ayat.molaa@fgs.stu.edu.iq , mohw2016@stu.edu.iq
Received: 29 December 2022; Accepted: 23 February 2023; Published: 2 July 2023

Abstract

This study investigated the performance of symmetric airfoils of type NACA0012 numerically under different operating conditions. It has been assumed that the study involves steady state, non-compressive, and turbulent flows. The operating fluid was air. The effect of Reynolds number and angle of attack on lift and drag coefficients, pressure distribution, and velocity distribution was investigated. ANSYS FLUENT has been used to solve the numerical model by using continuity equations, Navier-Stokes equations, and the appropriate K-ω SST perturbation model. This study shows a clear difference between the pressure coefficient of the lower and upper surfaces of the airfoil at high Reynolds numbers, indicating higher lift at high Reynolds numbers. As the maximum stall angle of the airfoil NACA0012 is 14° after which it decreases significantly, a direct relationship was observed between lift and drag coefficients and angle of attack.

Keywords: Airfoil, NACA0012, Numerically, Turbulent flow, Angle of attack, Drag coefficient, Lift coefficient.

https://doi.org/10.33971/bjes.23.1.11

1. Introduction

In the field of dynamics, aerodynamics is the study of the forces responsible for the motion of objects as they are influenced by their positions. There are a number of applications of low Reynolds number aerodynamics in the military and civil sectors, including gliders, wind turbines, small aerial vehicles (MAVs), and unmanned aerial vehicles (UAVs). It is the shape of an airfoil to provide the best lift for the least amount of drag, for an airfoil has a rounded leading edge, which is elongated to give a gradual curve in the direction of flow. Moving through the fluid to generate aerodynamic force, an airfoil provides the best lift for the least amount of drag. In terms of fluid dynamics, the study of airfoils is one of the fields that is of vital scientific significance. There are many examples of airfoils in a wide range of machines, including aircraft vertical stabilizers, submarine fins, rotary wings, and even some fixed wings, such as propeller blades, windmill blades, compressor blades, turbine blades in jet engines, and compressor blades in water cylinders. Because airfoils are streamlined, they can be either symmetrical or asymmetrical in shape because they are streamlined. CFD has been used in this study in order to analyze a symmetric airfoil NACA0012 numerically.

According to Koshy and Jacob [1], numerical simulations have been used to investigate the characteristics of flow around two airfoils, symmetric airfoil NACA 0012 and asymmetric airfoil NACA 2424. It has been concluded that the flow behavior of the two airfoils as well as the pressure distribution is similar, except when the angle is 0°, where the pressure distribution on the symmetry airfoil is similar while on the asymmetric airfoil is variable. It is evident that the angle of attack and coefficient of lift are related directly to each other as the angle of attack increases. Sadikin et al. [2] achieved a numerical simulation of a NACA0012 airfoil by using three different turbulence models, Spalart Allmaras, k-Realizable and k-ω SST models. As a consequence of the separation of a flow from a leading edge to a trailing edge, it has been reported that lift decreases and drag increases. There is a good correlation between the results of the three turbulence models and the results of previous studies that have been carried out. Martínez-Aranda et al. [3] conducted an experiment to study the effect of angles of attack and Reynolds numbers on the airfoil NACA0012 using the wind tunnel device. There are slight differences in the coefficients of lift and drag in the various Reynolds numbers in comparison to previous studies which is observed when the Reynolds number is increased, as well as a slight difference in the coefficients of drag for each Reynolds number when compared to previous studies. Singh [4] conducted an experimental study on the NACA0012 airfoil. Observe that there are values associated with the pressure coefficient. There are positive values on the upper surface and negative values on the lower surface, which in turn generate lift on the upper surface. Raval et al. [5] studied the numerical analysis of the NACA0012 airfoil. It was concluded that as the angle of attack increases, the lift coefficient will increase linearly, while the drag coefficient will increase gradually until the stall angle is reached. Kumar [6] used the k-ω SST turbulence model to explain the flow behavior of the NACA0012 airfoil. concluded that there is a direct relationship between the angle of attack and the lift coefficient. Show the pressure distribution on the two surfaces of the airfoil at zero

angles of attack as well as the velocity distribution at zero angles of attack for the two surfaces of the airfoil. Mallela et al. [7] studied the aerodynamics of the NACA0012 airfoil at angles of attack that were negative and positive and found that in both cases, pressure and velocity on the surface of the airfoil exhibited an inverse relationship at negative angles of attack, as well as the opposite at positive angles. Paper and Muramatsu [8] presented an experimental study investigating the influence of Reynolds number on pressure distribution and bubble separation behavior of a NACA 0012 airfoil with three different Reynolds numbers in accordance with the latest technology. Kabir et al. [9] investigated the influence of angle of attack and Mach number on the efficiency of the NACA 0012 airfoil, using a numerical model. The authors conclude that the pressure difference below and above the trailing edge of the airfoil, as well as the formation of vortices, is due to the increasing angle of attack of the airfoil. Initially, the flow speed at the entrance is subsonic, but as soon as it crosses the throat, the flow speed surpasses sound speed. Based on the flow analysis of two winglets (NACA 0012 and NACA 4412). Shahariar [10] observed that the pressure distribution of the upper and lower surfaces of the wing of NACA4412 is greater than that of that of NACA0012, which results in a higher lift than NACA0012. A numerical simulation of turbulent flow was carried out by Sahoo and Maity [11] for wings (NACA 0012 and NACA 4412, S809), and the NACA 4412 airfoil resulted in a higher lift coefficient than both NACA 0012 and S809 due to its thin outer profile and camber height. In 2018 [12], the dynamic properties of the NACA 0012 airfoil with different Reynolds numbers were demonstrated experimentally and numerically by Jha et al. Yousefi and Razeghi [13] studied the effect that Reynolds number and angle of attack have on the location of the turbulent-laminar transition based on Reynolds number and angle of attack. As the angle of attack increases. They found that with an increase in the angle of attack, the point of transition moves towards the leading edge of the airfoil. It has been demonstrated that the critical Reynolds number refers to the velocity at which the laminar flow above the airfoil ceases to exist. Kim et al. [14] conducted an experimental study and a numerical study to examine the boundary layer properties and the aerodynamic properties of the NACA0012 airfoil at low angles of attack in order to formulate a model. In the range of low Reynolds numbers, the sudden increase in lift coefficients is thought to be the result of boundary layer formation. This is the main reason for the sudden rise in lift coefficients. Nožicka et al. [15] studied numerically the aerodynamic performance of NACA4412 airfoil with the presence of Gurney flap at sizes (0.5 %, 1.0 %, 1.25 %, 1.5 %, 2.0 %, and 3.0 %). Concluded that the Gurney flap causes a significant increase in the lift coefficient with a slight increase in the drag coefficient if the size of the Gurney flap does not exceed 1.25 %. Almusawi et al. [16] numerically investigated the flow behavior of a NACA0012 semicircular groove airfoil. It was found that the semicircular groove increases the lift coefficient by 2.25 %, while the drag coefficient decreases by 4.32 % compared to the smooth airfoil.

Despite many previous research and studies that dealt with the issue of aerodynamics on the surface of the airfoils and the NACA0012 airfoil, some significant parameters have not been studied in detail, including the angle of attack, the low Reynolds number, and the pressure distribution. Since most of them were concerned with clarifying the effect of only one parameter, such as the low Reynolds number or angle of attack. In the current research, the focus is on studying what previous studies overlooked so that a wider range of low Reynolds numbers (8×10^4, 2×10^5, 3×10^5, and 4×10^5) was taken, as well as the angle of attack (0°-18° by 2 steps) and its effect on the lift and drag coefficients, also the pressure and velocity distribution on the airfoil. The collection of lift and drag coefficients and pressure distribution curves in one study gives manufacturers a more complete understanding of the aerodynamics at the surface of the airfoil and helps them design more efficient and high-performance airfoils.

2. Numerical study

In the present study, the ANSYS FLUENT 2021 R1 tool package was used to simulate the flow of fluids with various Reynolds numbers (8×10^4, 2×10^5, 3×10^5, and 4×10^5). This airfoil has a three-dimensional shape, and the flow in the airfoil is stationary and incompressible. This is done using the k-ω SST turbulence model, which is designed for low Reynolds number flows, and which excels in a high convergence rate and behavior when compared to other turbulent models in opposite pressure gradients and separating flows, which also require a computer with limited memory.

Using the NACA 0012 symmetric airfoil (non-camber) consists of four numbers in the NACA series and indicates that the airfoil does not have any camber, and the number (12) indicates that the thickness of the airfoil is 12 % of the chord length of the airfoil.

2.1. Mathematical model

It is significant to note that the first step in the numerical analysis consists of developing a mathematical model, which includes integral equations and boundary conditions. A continuity equation and a momentum equation are the foundation of these equations.

The 3D continuity and momentum equations, in general, can be written as follow [17]:

$$\nabla \cdot \vec{V} = 0 \tag{1}$$

x - direction

$$\rho(\bar{u}\frac{\partial \bar{u}}{\partial x} + \bar{v}\frac{\partial \bar{u}}{\partial y} + \bar{w}\frac{\partial \bar{u}}{\partial z}) = -\frac{\partial \bar{p}}{\partial x} + \mu\nabla^2\bar{u} + \bar{F}(turb, x) \tag{2}$$

y - direction

$$\rho(\bar{u}\frac{\partial \bar{v}}{\partial x} + \bar{v}\frac{\partial \bar{v}}{\partial y} + \bar{w}\frac{\partial \bar{v}}{\partial z}) = -\frac{\partial \bar{p}}{\partial y} + \mu\nabla^2\bar{v} + \bar{F}(turb, y) \tag{3}$$

z - direction

$$\rho(\bar{u}\frac{\partial \bar{w}}{\partial x} + \bar{v}\frac{\partial \bar{w}}{\partial y} + \bar{w}\frac{\partial \bar{w}}{\partial z}) = -\frac{\partial \bar{p}}{\partial z} + \mu\nabla^2\bar{w} + \bar{F}(turb, z) \tag{4}$$

Using ANSYS FLUENT, a NACA0012 airfoil model is created in the model's designer by selecting the parameters shown in Table 1 and creating a domain section test of 305 mm wide, 600 mm long, and 305 mm high. Also, the boundary conditions shown in Fig. 1 are selected. This is the boundary condition which is set as follows:

- *Inlet section:* The inlet is set at velocity (8.08, 20.21, 30.31, and 40.42 m/s).
- *Outlet section:* The outlet is set at zero pressure.
- The wall condition is set to no slip.

Where (ρ) is air density, ($\bar{u}$, $\bar{v}$ and $\bar{w}$) are velocity compounds in the direction (x, y and z) respectively. ($\bar{P}$) is pressure, (μ) is Kinematic viscosity, (∇) dl operator, ($\vec{V}$) is velocity vector, and ($\vec{F}$) is external force acting on the fluid.

Table 1. Dimensions of the airfoil.

Chord (C)	0.15 m
Span (S)	0.3 m
Area (A)	0.045 m^2

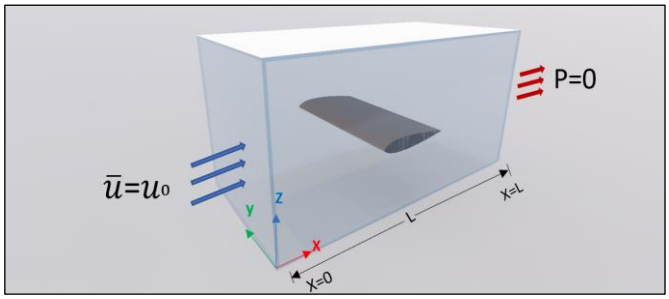

Fig. 1 schematic diagram of airfoil.

2.2. Mesh

The meshing of the NACA0012 airfoil simulator was constructed using ANSYS FLUENT according to Fig. 2 and with input parameters as in Table 2.

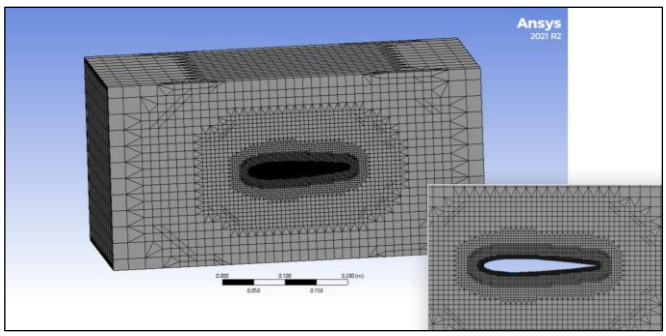

Fig. 2 Mesh for airfoil (NACA0012) and airfoil domain.

Table 2. Mesh parameters.

Parameters	Values
Number of nodes	2802362
Number of mesh elements	2675103
Maximum aspect ratio	2.798
Minimum orthogonal quality	0.9533

2.2.1. Mesh independence test

As a result of using a large number of mesh elements, we can achieve a more accurate numerical solution. However, the drawback of using a larger number of mesh elements is the requirement for a large amount of computer memory and lengthy computation time. To verify the influence of mesh size on numerical simulation, Hexahedron mesh in five sizes is chosen to obtain accurate results. This was done with a suitable amount of computer memory and a reasonable amount of time. The ratio (C_L / C_D) was plotted and analyzed in relation to different angles of attack (0°-18° by 2 steps) at a Reynolds number of (8×10^4). According to the results of the grid independence test shown in Fig. 3, it appears that three mesh types of elements (1034566, 1343782, 2246431, 2676481, 3476882) were almost similar in terms of results, but took a different amount of time to calculate. As a result, the number of mesh elements (2676481) was selected because it produces accurate results with an adequate amount of memory on the computer.

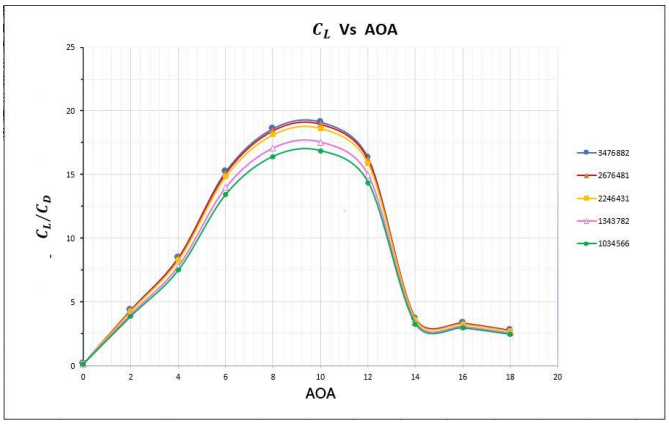

Fig. 3 Mesh independence.

2.3. Setting up FLUENT

In Fluent, the geometry and mesh are brought in as well as the initialization and solver are applied. During low-viscosity fluid flows, turbulent flow is created by increases in kinetic energy causing unstable vortices of various sizes to form due to the increased kinetic energy in parts of the flow. As a result, the coupled method (pressure-velocity coupling) was chosen. It has been decided that Least Squares Cell Based will be used in the spatial discretization section. The Second Order Upwind was used to solve the momentum, the First Order Upwind was used to solve the turbulent dissipation rate and turbulent kinetic energy, and the simulation parameters are also used in Table 3 to get accurate results. During initialization, the program runs a series of calculations before performing the actual calculation.

Table 3. Input data for FLUENT simulation.

Parameters	Values
Viscous model	k-ω SST (2 equations)
Operating temp.	293 (K)
Operating pressure	0.0 (Pa)
Density of fluid	1.204 (kg/m^3)
Kinematic viscosity	1.825×10^{-5} (kg/m.s)
Angle of attack	(0° - 18° by 2 steps)
Force monitor	Lift and drag
Fluid	Air is the ideal gas

3. Validation

To confirm the reliability and accuracy of the numerical results of the current paper. Investigated the numerical results of the Patel and Thakor [6] using the ANSYS FLUENT program, where the results were compared for the lift and drag coefficients of a symmetric NACA0012 airfoil (chord length

= 1 m) at the angles of attack (0, 3, 5, 8, 11, 13, 16, and 18) degrees and the velocity of air 30 m/s as shown in Figs. 4 and 5. The results of this study showed a high degree of agreement and reliability with those of the Patel and Thakor, where the code can be used in the study.

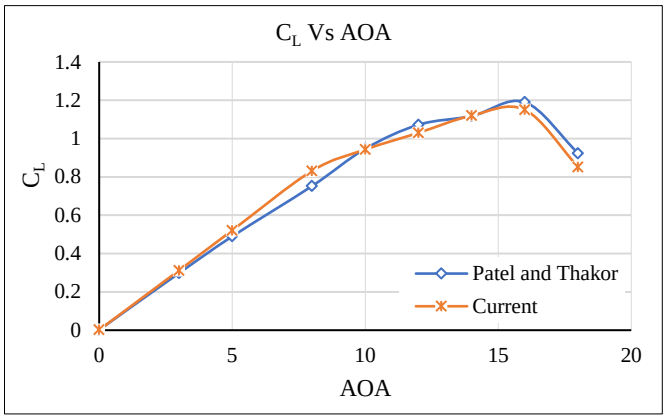

Fig. 4 Validation of C_L Vs Angle of attack.

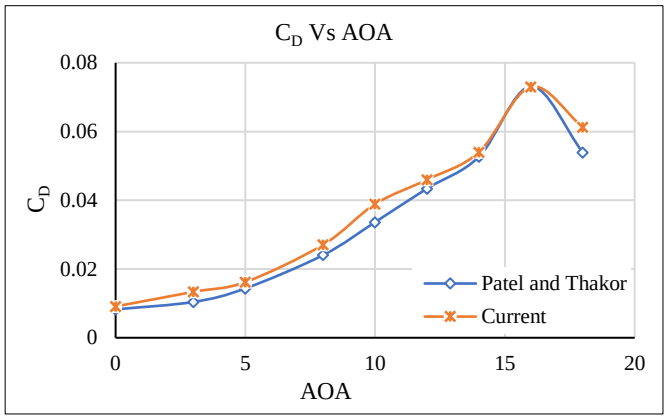

Fig. 5 Validation of C_D Vs Angle of attack.

4. Results and discussion

4.1. Pressure and velocity distribution

Figures 6 - 9 show the distribution of pressure and velocity around the airfoil. At an angle of attack of 0, it shows that there is symmetry in the distribution of pressure and velocity on the upper and lower surfaces of the airfoil. This is because the airfoil has zero camber. Increasing angles of attack lead to a difference in pressure and velocity around the airfoil. This is because the pressure increases towards the lower surface and decreases at the upper surface of the airfoil. In contrast, flow velocity increases at the upper surface and decreases at the lower surface of the airfoil. According to Bernoulli's principle, fluid pressure drops when velocity rises, and vice versa. As the angle of attack continues to increase, the airflow begins to separate and moves toward the leading edge of the airfoil at the critical angle of attack (stall angle). The stall angle is 12° at the Reynolds numbers (8×10^4, 2×10^5, and 3×10^5), while it is at 14° at the Reynolds number (4×10^5). The separation of the flow stream causes the formation of vortices that lead to the occurrence of chaos and turbulence, and thus the flow stream loses its lamellar properties. This phenomenon is called stalling.

Figure 10 (a), (b), and (c) shows the variation in pressure coefficient (Cp) at various angles of attack for the NACA0012 airfoil with Re = 8×10^4. It is observed that the pressure distribution on the airfoil from the leading edge to the trailing edge is gradual. This is because the difference in pressure coefficient at the leading edge is much higher than that at the trailing edge. The leading edge of the airfoil generates most of the lift, thus indicating that this is where the lift begins. According to the normalized chord length, the pressure coefficient curves of the two surfaces of the airfoil coincide and possess positive and negative values. This is due to the symmetric geometry of the airfoil, see Fig. 10 (a). Once the stall angle reaches 12°, the difference in the pressure coefficient between the two surfaces of the airfoil increases dramatically. The difference in the pressure coefficient at the trailing edge of the airfoil is less than that at high angles of attack. This is because the pressure coefficient at the lower surface decreases more than at the surface at high angles of attack. Flow separation is indicated by the upper, where vortices extend along the surface of the airfoil. The pressure coefficient difference between the lower and upper surfaces of the airfoil increases as the Reynolds number increases at all angles of attack and with the same behavior, see Fig. 11 (a), (b), and (c), when the pressure coefficient difference for the two airfoil surfaces is (3.63 and 6.71) at Reynolds numbers (8×10^4 and 4×10^5), respectively.

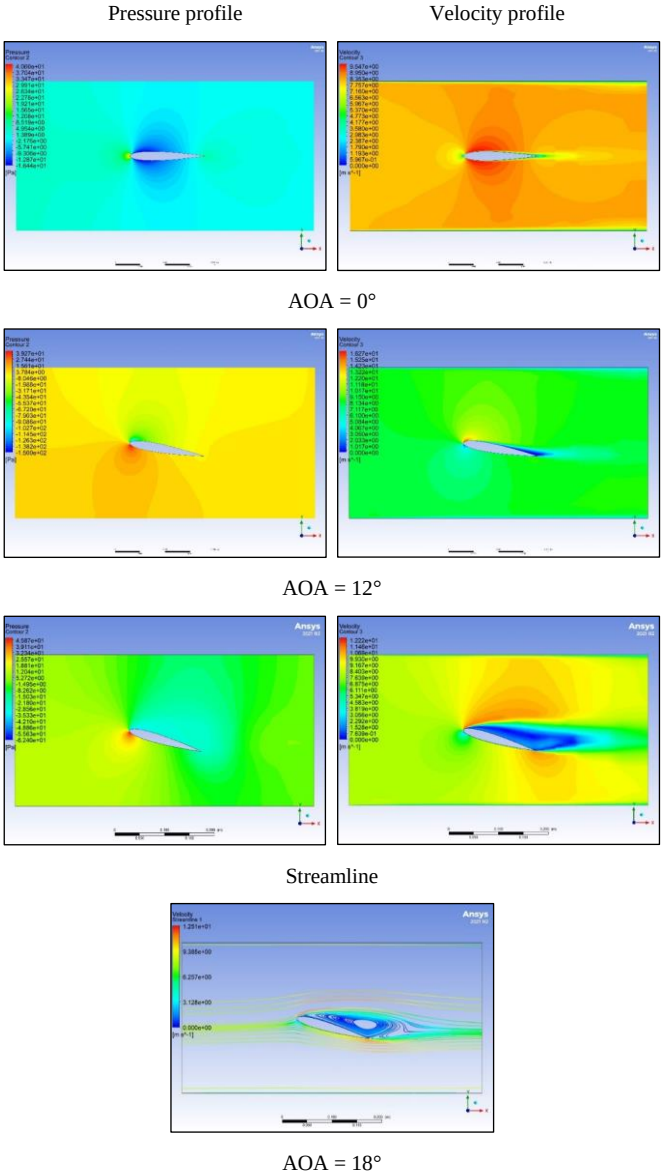

Fig. 6 Distribution of pressure and velocity profiles with streamline around the airfoil NACA0012 using different angles of attack at Re = 8×10^4.

Pressure profile Velocity profile

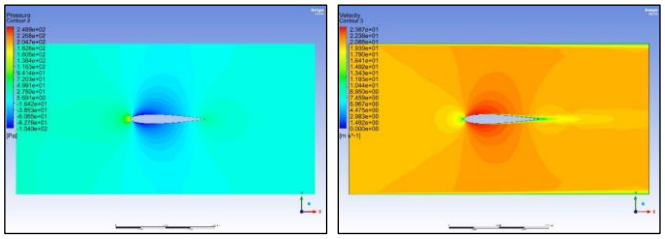

AOA = 0°

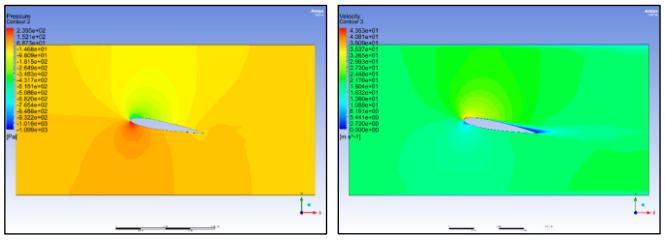

AOA = 12°

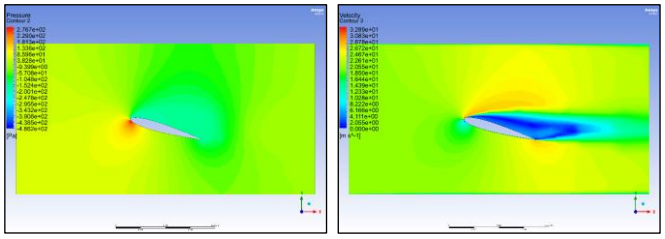

Streamline

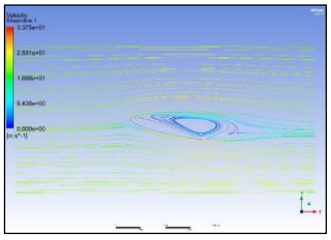

AOA = 18°

Fig. 7 Distribution of pressure and velocity profiles with streamline around the airfoil NACA0012 using different angles of attack at Re = 2×10^5.

Pressure profile Velocity profile

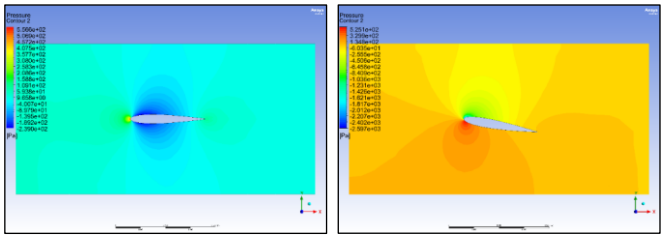

AOA = 0°

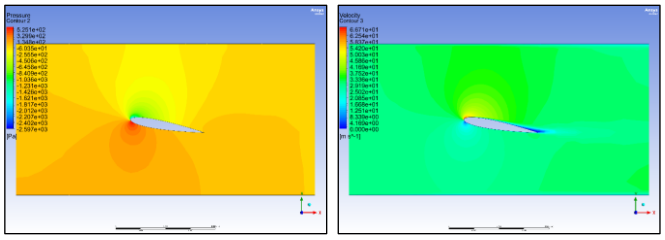

AOA = 12°

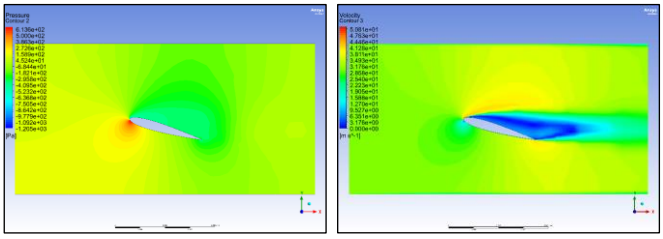

Streamline

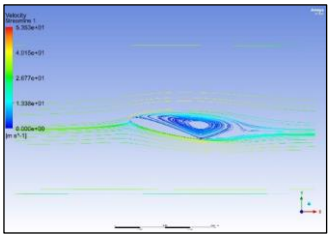

AOA = 18°

Fig. 8 Distribution of pressure and velocity profiles with streamline around the airfoil NACA0012 using different angles of attack at Re = 3×10^5.

Pressure profile Velocity profile

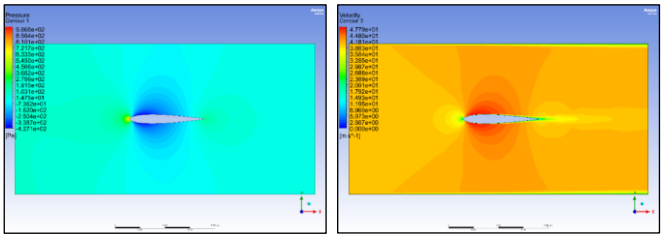

AOA = 0°

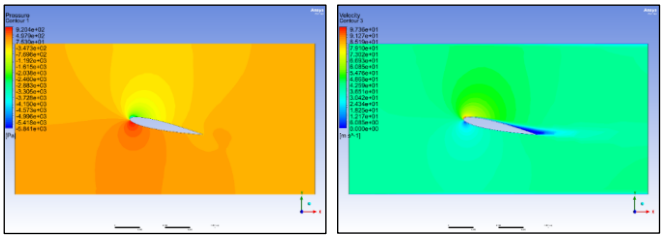

AOA = 14°

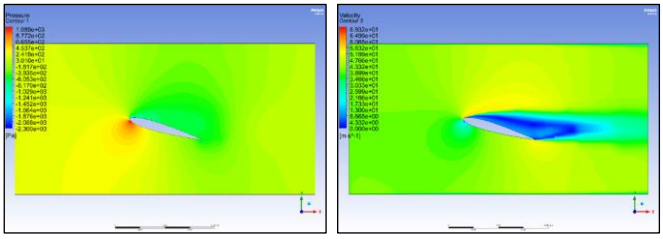

Streamline

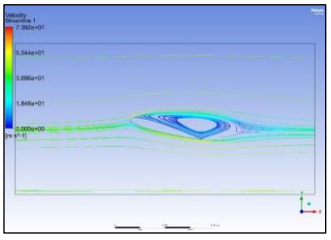

AOA = 18°

Fig. 9 Distribution of pressure and velocity profiles with streamline around the airfoil NACA0012 using different angles of attack at Re = 4×10^5.

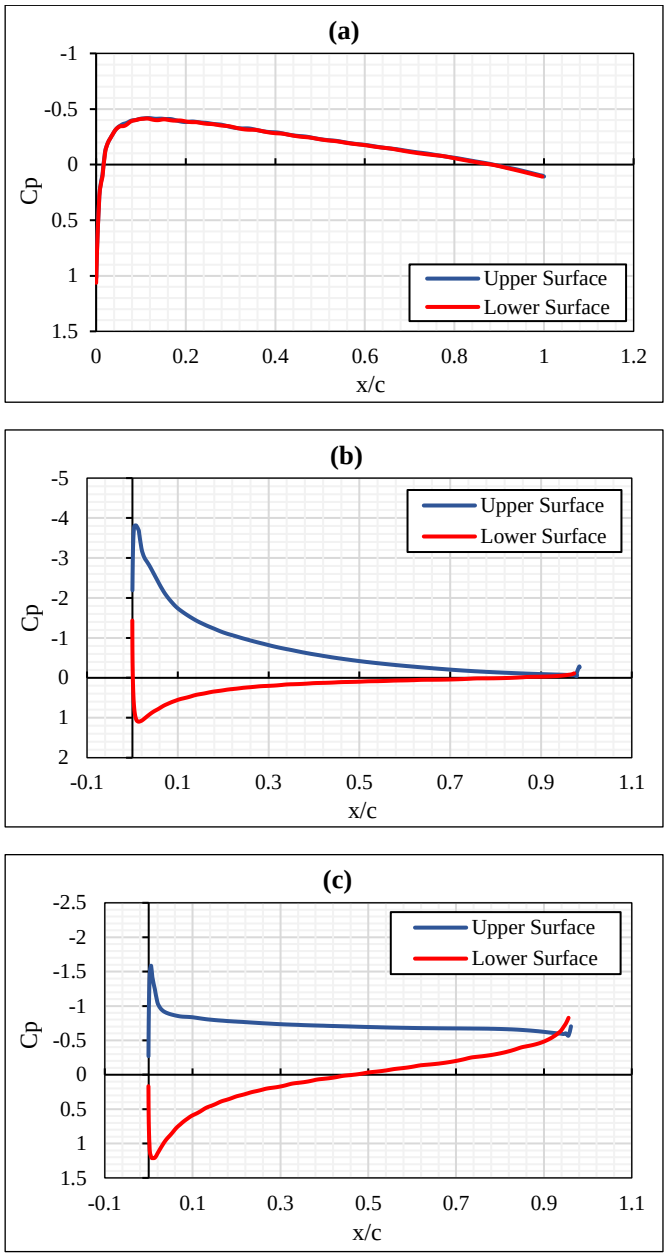

Fig. 10 Distribution of pressure coefficient around upper and lower surfaces to airfoil NACA0012 using Re = 8 × 10^4 at **(a)** AOA = 0°, **(b)** AOA = 12°, and **(c)** AOA = 18°.

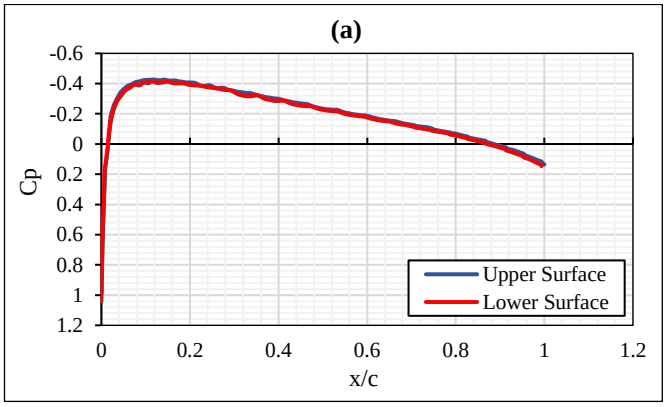

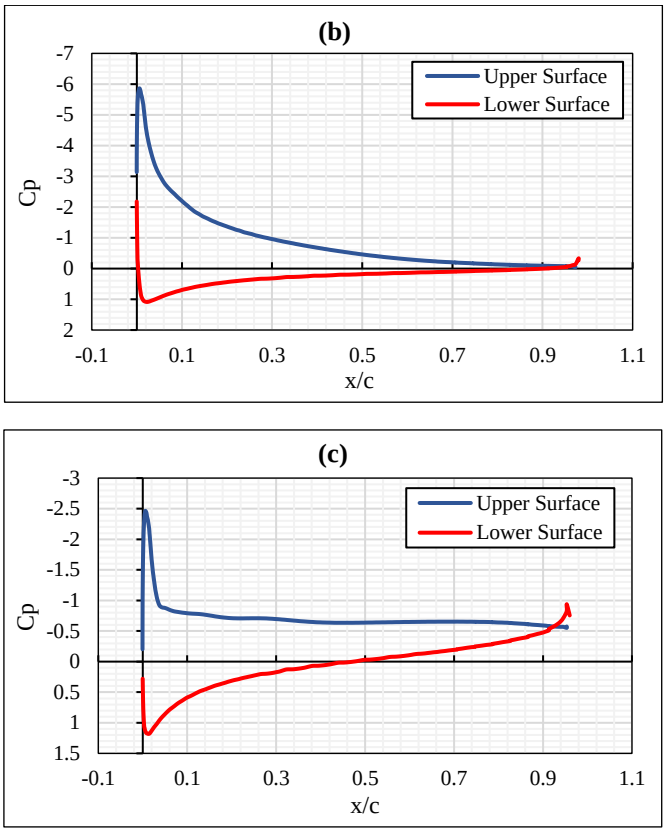

Fig. 11 Distribution of pressure coefficient around upper and lower surfaces to airfoil NACA0012 using Re = 4 × 10^5 at **(a)** AOA = 0°, **(b)** AOA = 14°, and **(c)** AOA = 18°.

4.2. Effect angle of attack on C_L and C_D

At different angles of attack, Figs. 12 and 13 show the lift and drag coefficients. Airfoils produce lift when the upper and lower surfaces have different pressures. At Reynolds numbers of eight, two, three, and four, the lift coefficient nearly quadruples when the angle of attack rises. Where it peaks at the stall angle 120 is at the Reynolds number (8 × 10^4, 2 × 10^5, and 3 × 10^5), and at the stall angle 140 is at the Reynolds number (4 × 10^5). The drag coefficient increases gradually until the stall angle is reached. As the angle of attack increases, the lift coefficient drops rapidly and suddenly, and the drag coefficient changes dramatically. The large gradient of opposite pressure causes the flow stream to separate and vortexes to form. At high angles of attack, the lift decreases and the drag increases as the velocity decreases and turbulence intensifies on the upper surface of the airfoil.

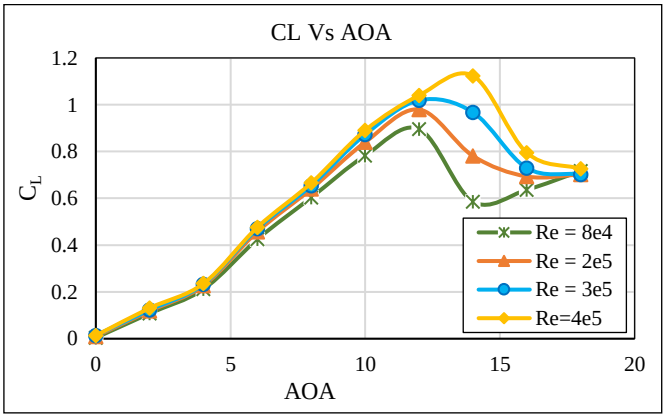

Fig. 12 Effect angle of attack on C_L at different Reynolds number.

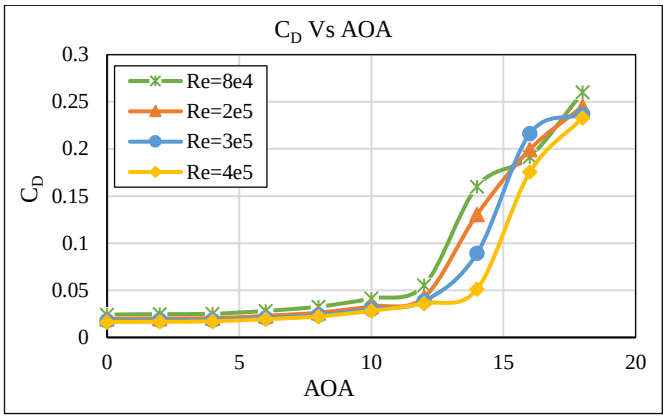

Fig. 13 Effect angle of attack on C_D at different Reynolds numbers.

4.3. Effect Reynolds number on C_L and C_D

As a ratio of inertial forces to viscous forces, the Reynolds number can be defined. As the Reynolds number increases, the coefficient of lift increases and the coefficient of drag decreases. As the Reynolds number increases, the airfoil stall angle increases due to the delay in flow separation as the angle of attack increases, Figs. 14 and 15. As a result of the small change in the location of the turbulent laminar transition, this effect of the Reynolds number is of small significance when comparing the aerodynamic properties of different low Reynolds number systems.

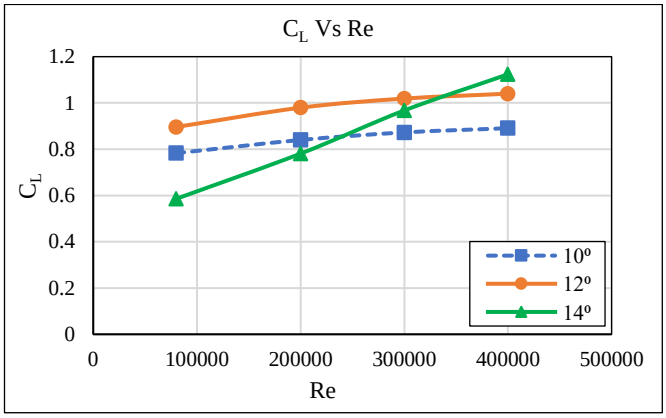

Fig. 14 Effect Reynolds number on C_L at an angle of attack (10°, 12°, and 14°).

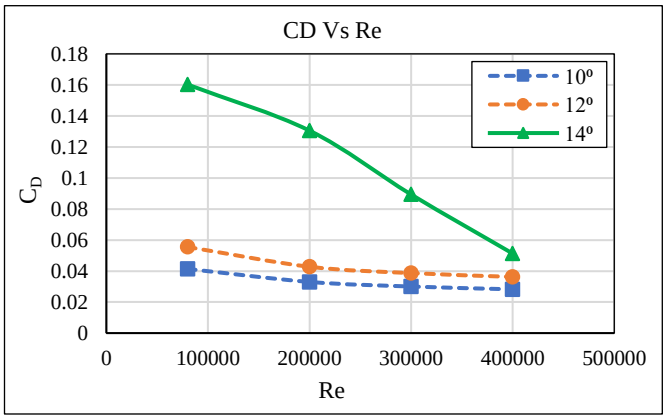

Fig. 15 Effect Reynolds number on C_D at an angle of attack (10°, 12°, and 14°).

4.4. Effect angle of attack and Reynolds number on C_L/C_D ratio

Designing an aircraft to produce lift is not enough. The aircraft must achieve a high L/D ratio in order to increase its range and overcome its weight. The ratio L/D or C_L/C_D is the value of the lift produced by the airfoil against the value of the drag generated by its movement through the air. This is described as the efficiency of the airfoil. The L/D ratio is directly proportional to the Reynolds number and the angle of attack until it reaches the stall angle, Figs. 16 and 17. With an increase in the angle of attack and the separation of the flow stream, the L/D ratio decreases. This is due to the sudden drop in the lift coefficient and the maximum increase in the drag coefficient.

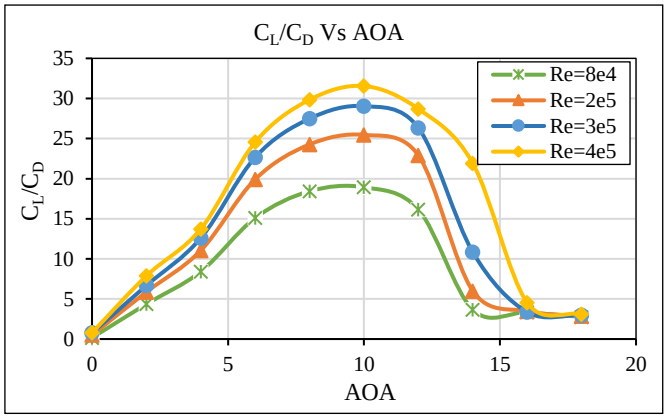

Fig. 16 Effect the angle of attack on C_L/C_D ratio at different Reynolds numbers.

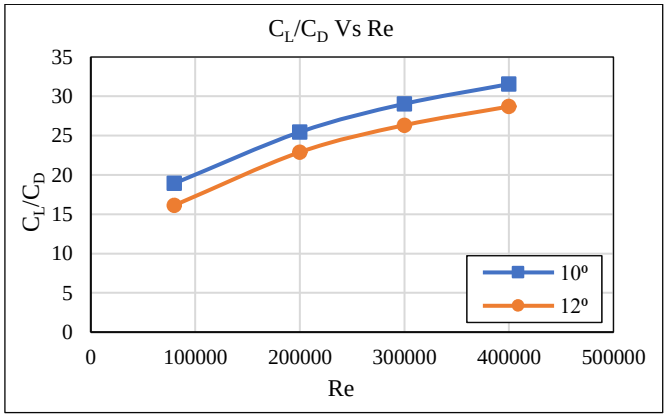

Fig. 17 Effect Reynolds number on C_L/C_D ratio at an angle of attack (10°, 12°).

5. Conclusions

In the present paper, a numerical study was conducted by CFD of a symmetric airfoil NACA0012 in which the k-ω SST turbulence model was used with different angles of attack and low Reynolds numbers for several parameters. As a result of the search, the following results were found:

1. The NACA0012 airfoil produces zero lift due to an even distribution of pressure and velocity on the two surfaces.
2. With the increase in the angle of attack, the lift coefficient increases almost linearly until it equals the angle of 12° for the Reynolds numbers (8×10^4, 2×10^5, and 3×10^5) and 14° for the Reynolds numbers (4×10^5). Where the lift coefficient reaches its maximum value, while the drag coefficient increases it reaches the stall angle.

3. As a result of the continuous increase in the angle of attack, a difference in pressure and velocity occurs around the two surfaces of the airfoil. The pressure increases and the velocity decreases at the upper surface and vice versa at the lower surface. This causes the separation of the airflow and the formation of vortices that increase the intensity of turbulence. Therefore, the lift coefficient decreases, and the drag coefficient increases suddenly and quickly.
4. At a lower Reynolds number, the stall angle increases, the lift coefficient increases, and the drag coefficient decrease because the flow separates more slowly.
5. The ratio (C_L/C_D) is positively affected by an increase in the low Reynolds number and the angle of attack until it reaches the stall angle. Increasing the angle of attack weakens the performance of the airfoil. This is due to the simultaneous increase in drag force and decrease in lift force.

Symbols and Acronyms		
Symbols	**Description**	**SI Unit**
L	Lift force	N
D	Drag force	N
C_L	Lift coefficient	--
C_D	Drag coefficient	--
Cp	Pressure coefficient	--
Re	Reynolds number	--
P	Pressure	N/m^2
C	Chord length	m
$\bar{u}$	Velocity compounds in the direction (x)	m/s
$\bar{v}$	Velocity compounds in the direction (y)	m/s
$\bar{w}$	Velocity compounds in the direction (z)	m/s
$\bar{F}$	External force acting on the fluid	N
∇	Del operator	--
A	Wing surface area	m^2
$\vec{V}$	Velocity vector	m/s
Greek Symbols		
Symbols	**Description**	**SI Unit**
ρ	Air density	kg/m^3
ω	Turbulence energy dissipation frequency	s^{-1}
μ	Kinematic viscosity	kg/m.s
Abbreviation		
Symbols	**Description**	**SI Unit**
AOA	Angle of attack	Degree
NACA	National advisory committee for aeronautics	--
SST	Shear stress transport	--
CFD	Computational fluid dynamics	--

References

[1] A. P. Kunjumon, F. M. Koshy, S. T. Jacob, and Sunildutt, "Determination of Pressure Coefficient Around NACA Airfoil", International Journal of Applied Engineering Research, Vol. 14, No. 14, pp. 81-87, 2019.

[2] A. Sadikin, N. A. M. Yunus, S. A. Abd Hamid, A. E. Ismail, S. Salleh, S. Ahmad, M. N. Abdol Rahman, S. Mahzan, and S. S. Ayop, "A Comparative Study of Turbulence Models on Aerodynamics Characteristics of a NACA0012 Airfoil", International Journal of Integrated Engineering, Vol. 10, No. 1, pp. 134-137, 2018. https://doi.org/10.30880/IJIE.2018.10.01.019

[3] S. Martínez-Aranda, A. L. García-González, L. Parras, J. F. Velázquez-Navarro, C. del Pino, "Comparison of the aerodynamic characteristics of the NACA0012 airfoil at low-to-moderate Reynolds numbers for any aspect ratio", International Journal of Aerospace Sciences, Vol. 4, No. 1, pp. 1-8, 2016. https://doi.org/10.5923/j.aerospace.20160401.01

[4] M. Singh, "Fabrication and Analysis of NACA 0012 Airfoil in Wind Tunnel", International Research Journal of Engineering and Technology (IRJET), Vol. 5, Issue 5, 2018.

[5] N. P. Raval, M. Malay, and L. Jitesh, "CFD Analysis of NACA0012 Aerofoil and Evaluation of Stall Condition", International Journal of Engineering Technology Science and Research, Vol. 4, Issue 4, pp. 57-60, 2017.

[6] P. Kumar, and J. Saini, "Numerical Analysis of Air Cooled Condenser using Cfd", International Journal of Scientific Research and Engineering Trends, Vol. 6, Issue 6, pp. 3577-3581, 2020.

[7] G. Mallela, P. Paturu, and M. Komaleswarao, "Lift and drag performance of NACA0012 airfoil at various angle of attack using CFD", International Journal of Mechanical and Production Engineering Research and Development (IJMPERD), Vol. 8, Issue 3, pp. 89-100, 2018. https://doi.org/10.24247/ijmperdjun201810

[8] Y. Yamaguchi, T. Ohtake, A. Muramatsu, "1201 Pressure Distribution on a Naca0012 Airfoil at Low Reynolds Pressure", 4th International Conference on Jets, Wakes and Separated Flows, ICJWSF2013, Nagoya, Japan, September 17-21, 2013. https://doi.org/10.1299/jsmeicjwsf.2013.4._1201-1_

[9] A. Kabir, M. Hasan, and Y. M. Akib, "Numerical Analysis on Naca 0012 Airfoil at Different Mach Numbers with Varying Angle of Attacks Using Computational Fluid Dynamics", 5th International Conference on Engineering Research, Innovation and Education School of Applied sciences and Technology, SUST, Sylhet, pp. 1-6, 2018.

[10] G. M. H. Shahariar, "Numerical Analysis and Comparison on Aerodynamics Characteristics on NACA-0012 & NACA-4412", International Conference on Mechanical, Industrial and Energy Engineering 2014, Khulna, Bangladesh, 26-27 December, 2014.

[11] S. Sahoo and S. Maity, "CFD Analysis of Responses of Two-Equation Turbulence Models for Flow over NACA 0012, NACA 4412 and S809 Aerofoils", Advances in Mechanical Engineering, Lecture Notes in Mechanical Engineering, Springer, Singapore, pp. 31-40, 2020. https://doi.org/10.1007/978-981-15-0124-1_4

[12] S. Jha, U. Gautam, S. Narayanan, and L. A. Kumaraswami Dhas, "Effect of Reynolds Number on the Aerodynamic Performance of NACA0012 Aerofoil", IOP Conference Series: Materials Science and Engineering, Vol. 377, Issue 1, 2018. https://doi.org/10.1088/1757-899X/377/1/012129

[13] K. Yousefi and A. Razeghi, "Determination of the Critical Reynolds Number for Flow Over Symmetric NACA Airfoils", AIAA American Institute of Aeronautics and Astronautics, 2018 AIAA Aerospace Sciences Meeting, pp. 1-11, 2018. https://doi.org/10.2514/6.2018-0818

[14] D-H. Kim, J-W. Chang, and J. Chung, "Low-Reynolds-Number Effect on Aerodynamic Characteristics of a NACA 0012 Airfoil", Journal of Aircraft, Vol. 48, No. 4, pp. 1212-1215, 2011. https://doi.org/10.2514/1.C031223

[15] J. Nožicka, M. Matejka, and P. Bárta, "PIV investigation of an airfoil with a Gurney flap", ICAS 2006, Edinburgh: UK on behalf of Counsel of the Aeronautical Sciences (ICAS), Vol. 2, pp. 1035-1040, 2006.

[16] M. S. Almusawi, Q. A. Rishack, and M. A. Al-Fahham, "Effect of Spanwise Semicircular Groove on NACA 0012 Airfoil", Vol. 22, No. 2, pp. 23-26, 2022. https://doi.org/10.33971/bjes.22.2.4

[17] J. M. C. Yunus A. Çengel, Fluid Mechanics: Fundamentals and Applications, McGraw-Hill series in mechanical engineering, 2006. ISBN 0-07-247236-7